International Journal of Mechanics Structural.
ISSN 0974-312X Volume 4, Number 1 (2013), pp.1-23

http://www.irphouse.com

Contribution to the Characterisation of the Coconut Shells (Coco Nucifera) of Cameroon

E. Njeugna[(1)] ; D. Ndapeu[(1) (2)] ; S. Bistac[(3)] ; J.Y.Drean[(4)] ; J. Ngenefeme Foba[(5)] and M. Fogue [(2)]

(1) Laboratoire de mécanique et de Matériaux adaptés.
ENSET-university of Douala-Cameroon
(2) Laboratoire d'Ingénieurie des Systèmes Industriels et de l'Environnement
IUT FV de Bandjoun-University of Dschang - Cameroon
(3) Laboratoire de Photochimie et d'Ingénierie Macromoléculaires.
Université de Haute Alsace-France
(4) Laboratory of Physics and Mechanical Textile ENSISA of MULHOUSE-France
(5) University of Buea-Cameroon

Abstract

This paper presents mechanical and physicochemical characteristics of two species of coconut (cocos nucifera) from Cameroon and the evaluation of their potential for use as reinforcing fillers in the preparation of composites. Physicochemical characterization was performed by FTIR, SEM and TGA. Observation under the electron microscope revealed that the physical structure of the coconut shell is granular with grains lengthened in the southernmost direction of nut. FTIR analysis revealed fingerprint peaks typical of cellulose and lignin. Thermo gravimetric analysis decomposition in three mass loss steps with low residual mass. Toughness was evaluated by measuring impact and this was evaluated as a function of temperature, for temperature between 25°C and 137°C. Tensile prospection was by three point bend test, from which Youngs' modulus and the Poisson ratio were determined. From the results obtained, we conclude that the coconut shell is an anisotropic material. Moreover the phenomenon of hysteresis was observed in these materials.

Key Words: coconut shells; impact energy; Young modulus; coconut nucifera; mechanical hysteresis.

1 INTRODUCTION

A good number of the plants in the world in general and Cameroon in particular, yield shells and the hard cores. These hard shells and cores, for the major parts, are not exploited and worse still are thrown in our immediate environment after consumption of their fruit causing pollution. For example, in the production of palm oil in Cameroon, the formal sector (SOCAPALM, CDC, PALMOIL) produced close to 200 000 tons per year and the considerable abstract sector, approximately produces 50 000 tons per year [1]. These two sectors have close to 300 000 tons of nut shells to palm trees of which nearly 70% are unexploited. The only form of exploitation in use is the form of fuel.

Taking into account their importance in the world economy in general and that of Cameroon in particular, certain plants with shells or hard cores deserve more attention in order to optimize the potentials that this waste represents. The coconut shells has been the subject of many investigations for the production of activated carbons [2,3,4,5,6], and some limited work has been done to establish its suitability for its use in composites [7,8,9,10,11] and as alternative granulate for concrete formulation[3]. The optimization of the use of these shells in the composites requires the knowledge of its physical, chemical and mechanical properties.

It is a question in this work of contributing to the mechanical and physio-chemical characterization of the coconut shells nucifera of Cameroon. The required objectives being the utilization of these shells like abrasive materials charges in the composites. The various aspects approached are the following:

- The physicochemical characterization of the coconut shells: this characterization will consist in determining their density, their structure, the volatile materials and the chemical composition;
- Their mechanical characterization: this characterization will consist in determining their energy of impact strength, their rheological parameters (Young modulus and Poisson's ratio).
- Finally the comparison of the results with other materials will locate us on the potential of the latter.

2 Materials and techniques

2-1 Material

The coconut shells used in this study come from the areas of the Littoral, the South and the South West of Cameroon. Two varieties of shells were concerned, and they are characterized by the form from their nut: a lengthened form (species 1) and a round form (species 2). The shells result from nuts in maturity and were preserved at the free air. These shells were delicately cleaned, as well on their inner and outer face, to remove the impurities before the preparation of the samples intended for the tests.

2-2 Techniques

2-1-1 Physicochemical Characterization

a. Density

To determine the absolutes densities of the two species of shells, a graduated test tube and a precision balance (CS 2000) were used to respectively measure volumes and the masses of the samples of shells. Water was introduced into the test tube until a given graduation, corresponding to the volume V_0, the sample unit + water was weighed, and its mass is noted m_o. The test tube containing water was placed on the balance, and a certain quantity of introduced shells; let us recall that these shells run in water. We can simultaneously read V' volume of the water level in the graduated beaker, and masses m' it posted by the balance. We then deduce the mass $m_i = m' - m$ and volume $V_i = V' - V_o$ from the sample of shell introduced into the graduated beaker. Several couples of experimental values (m_i, V_i) can thus be measured. The linear curve of regression $m = \rho V + B$ of these data by the method of least squares [12]. Figure 1 gives us the experimental curve mass-volume of species 1. The slope of the linear regression ρ represents the sought density.

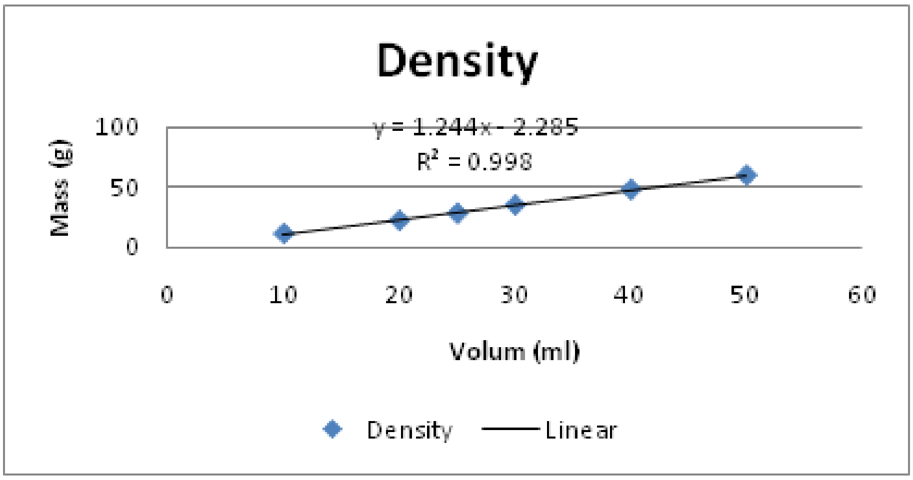

Figure 1: Experimental data and linear regression of masses in respect to the volume of the coconut shell species 1

b. Scanning Electron Microscopy (SEM)

The structure of coconut shells has been observed under electronic microscope using HITACHI S2360N.

c. FITR Analysis

The FR analysis carried out on the coconut shell using a FTIR spectrometer (Bruker Vertex 70) has been done. A ATR device was used. The analyses were performed with SO scan with a resolution of 4 cm^{-1}.

a. Thermo gravimetric analysis (TGA)

The Thermo gravimetric analysis of the coconut shell realized using a universal apparatus called TGA Q500 V20 with a temperature rate equal to 10°/min in nitrogene atmosphere.

2-1-2 Mechanical Characterization

This characterization aims at determining the energy of impact strength and the rheological parameters as the Young modulus and the Poisson's ratio. To be done, we carried out impact tests, elastic contact of Hertz and 3 points flexural tests, on samples taken from the coconut shell. The geometry of coconut shells presents two distinctive poles; moreover the behavior in the southernmost direction seems to be different from that in the equatorial direction. Figure 2 presents the description of the geometry of these shells as we will use in this article. With an aim of checking this anisotropy, with regard to the impact tests, we distinguished two zones from taking away of the samples: the polar zone (two poles) and the central zone, and in each zone us taken samples as well in the southernmost direction than equatorial. Table 1 gives us the typology adopted for the designation of the samples.

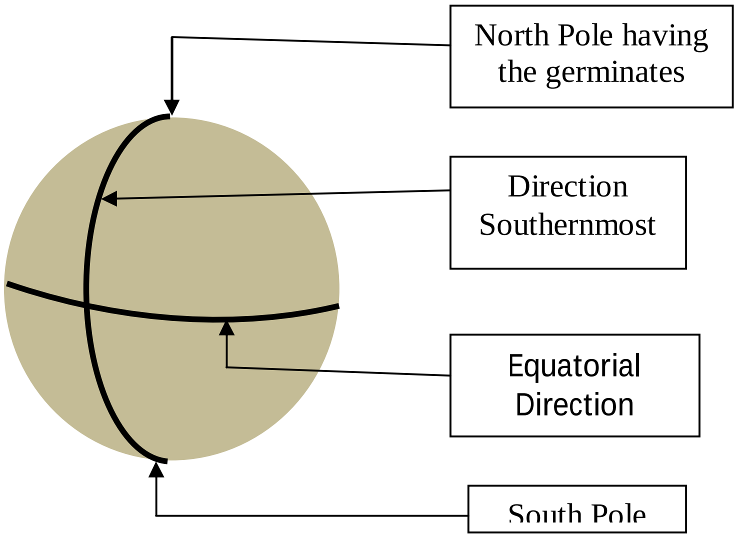

Figure 2: Geometry of coconut

Table 1: Various types of samples

Symbols	Designations
ZE-E	Sample obtained in the Equatorial Zone and Equatorial Direction
ZE-S	Sample obtained in the Equatorial Zone and Southernmost Direction
ZP-E	Sample obtained in the Polar Zone and Equatorial Direction
ZP-S	Sample obtained in the Polar Zone and the Southernmost Direction

As for the 3 points flexural tests, we took the samples in southernmost direction (S) and the equatorial direction (E).

a. Impact tests

The testing device of impact strength used is a "Mouton pendule" adapted to the vegetable shells conceived and carried out at the Laboratory of Mechanics and Adapted Materials (LAMMA), University of Douala whose figure 3 presents a photograph of this device.

Figure 3: photograph of the adapted Sheep Pendulum

This apparatus receives the prismatic samples of section 4×4 or 4×3 mm² and length going from 15 to 28 mm. In each zone and following the equatorial or southernmost direction, we cut 10 right samples which we tested.

We determined the evolution of the energy of impact strength of these shells according to the temperature. For that, we subjected samples to temperatures going of 25°C with 137°C by making 8 experimental points.

b. Determination of the Young modulus and Poisson ratio.

It is a question of determining the Young modulus and the Poisson's ratio of the matured coconut shell. This determination is made by exploiting the results obtained from the 3 points flexural tests and elastic contact of Hertz. But after all, it is sensible to know whether this material is ductile or brittle.

b-1 Static 3 points flexural test

b-1-1 Experimental device

According to the geometry curves of these shells; it is difficult to extract the right samples for standard tests. We could cut the samples having geometry curved of beam such as we can find in figure 4. The principle of the 3 points flexural test is illustrated on figure 5.

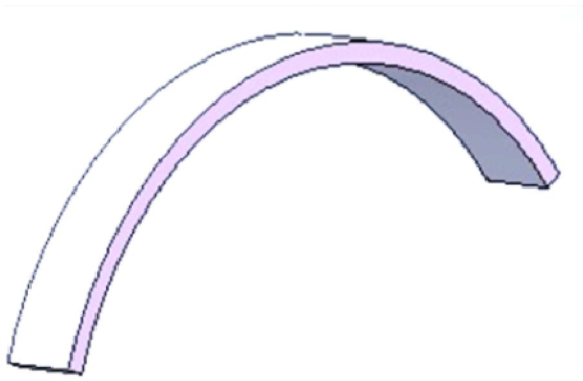

Figure 4: Geometry of test piece of flexural test

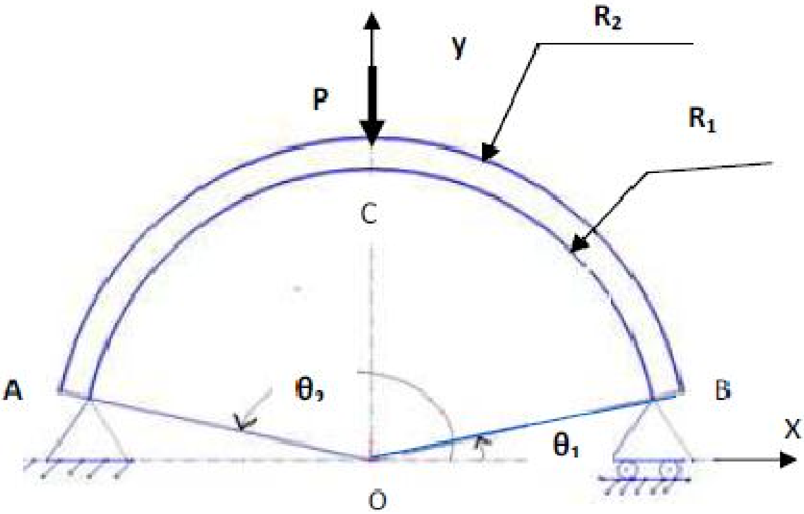

Figure 5: Principle of the 3 points flexural test

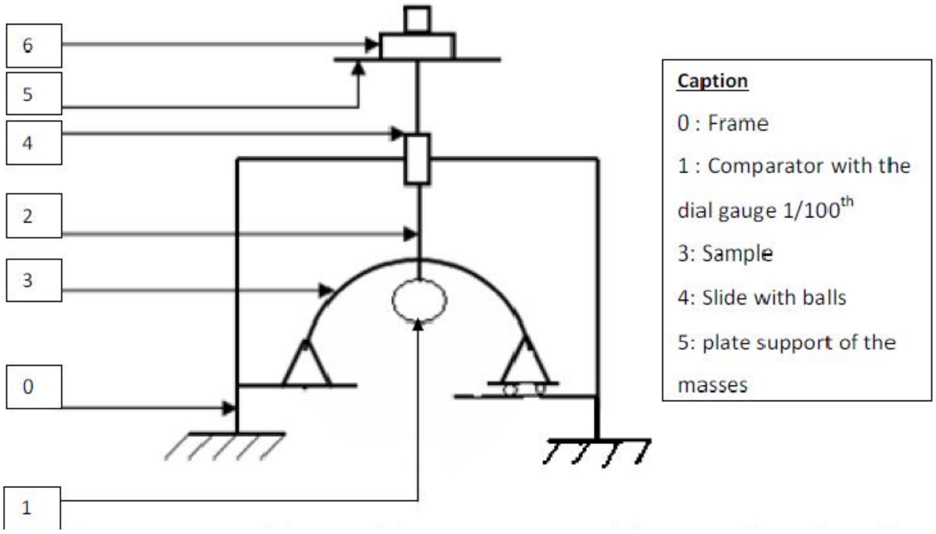

Figure 6: Functional diagram of the testing apparatus of the 3 points flexural test + legend

We designed and carried out a device for the flexural tests in statics of the curved beams. This device is schematized on figure 6 where sample 3 is laid out on the surface of supports related to frame 0, this bearing surface is made out of sufficiently thick steel sheet is perfectly rigid compared to the loads applied to neglect these deformations. The left end of the sample is made motionless, while its right end is free in translation in the horizontal direction. The plate with stem 6-2, guided in rectilinear translation movement in the vertical direction, compared to the frame, rests by the end of C on the centroid of the sample. The plate receives lead 6 used for the calibration of the effort. The feeler of the dial gauge with $1/100^{th}$, reference 1, laid out with the point C, under the sample, and in the prolongation of the stem of loading, is used to directly measure the arrow corresponding to a given load.

The experimental data-gathering for a sample, is done by the statement of the couples of values: charge P and corresponding arrow Y_C. We tested samples drawn from the two species of shell and cut as well in the southernmost direction as in the equatorial direction. Table 3 below gives us the number of samples tested by species and according to each direction.

b-1-2 Ductile Character of the coconut shell

To highlight the ductile character of this material, we carried out three points deflection tests, according to the principle mentioned above, until the rupture.

b-1-3 Experimental Data-gathering

We limited ourselves to the linear part of the curve of the 3 points deflection tests, to seek a relation between the Young modulus and the Poisson's ratio of this material. We thus tested samples coming from the two species of coconut and cut as well in the southernmost direction as in the equatorial direction. Table 2 gives us the number of test-tubes tested by species and according to each direction.

Table 2: Stamp distribution of the samples for the flexural test

species	Southernmost direction	Equatorial direction
1	8 samples	10 samples
2	8 samples	10 samples

The samples are indicated i X j where i indicates the species (1 or 2); X indicates the direction in which the sample is cut: Southerner (M); Equatorial E and j indicate the number of the sample. The data thus collected enable us to plot the experimental curves of deflection Y_C according to the load P in the elastic range of the shell; as well for the loading as for unloading. The figure 7 is that of sample 1E1.

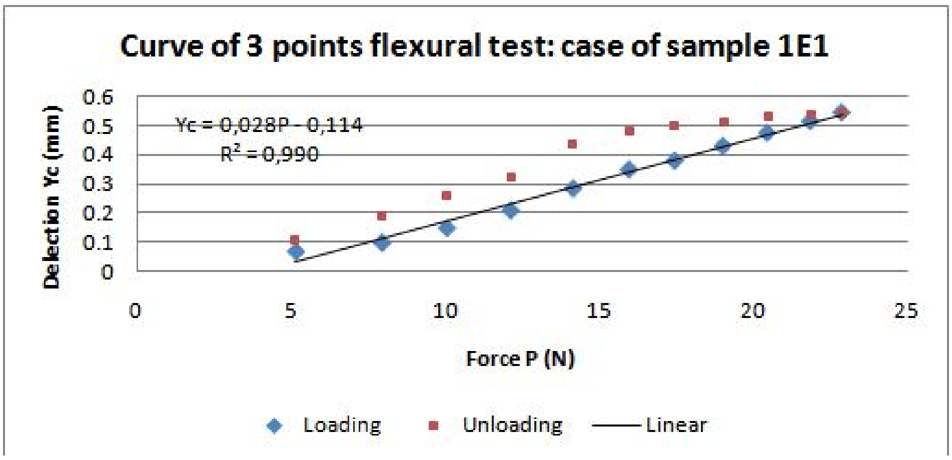

Figure 7: Curve of 3 points flexural test

The linear regression line gives us the relation $Y_C = a_1P$ where a_1 is the slope of this line.

b-1-2 Exploitation of the experimental data

To exploit these experimental data, we developed a mathematical model based on the calculation of the total energy of deformation due to the inflection of each sample. The application of the theorem of Castigliano [14] to the point C, gives us the linear relation between Y_C and P ; that is to say Y_C = a.P where "a" is a function not only of the geometry of the structure, but also of the mechanical characteristics such as the static Young modulus E and of the Poisson's ratio ν. The experimental relation $Y_C = a_1$ P and the theoretical relation Y_C = a.P make it possible to identify a_1 and a. Which enables us to have an equation with two variables (E and ν). We give the expression of a below but before, we specify the geometrical characteristics used in the mathematical model. Figure 13 gives us an illustration of the model.

In this model: R is the average radius; P the load. $2\theta_1 + \theta_2 = 180°$

a. Expression of the total energy of deformation of this beam (see appendix)

$$U = \frac{\mathrm{RP}^2}{8\mathrm{ES}}\left(\frac{\pi}{2}-\theta_1+\frac{1}{2}\sin 2\theta_1\right)+\frac{RP^2}{8GS}\left(\frac{\pi}{2}-\theta_1-\frac{1}{2}\sin 2\theta_1\right)+$$
$$\frac{\mathrm{R}^3P^2}{4EI_{Gz}}\left[\left(\frac{\pi}{2}-\theta_1\right)\left(\cos^2\theta_1+\frac{1}{2}\right)+\frac{3}{4}\sin 2\theta_1-2\cos\theta_1\right] \qquad 2.1$$

L and E are dimensions of the cross section: L is the width; E is the thickness;

- the area of the cross section is S=L.e 2.2
- E is the static Young modulus in the longitudinal direction ;
- ν is the Poisson coefficient;
- The static module in the transversal direction is: $\mathrm{G}=\frac{\mathrm{E}}{2(1+\nu)}$ 2.3
- P is the load apply;
- The quadratic moment of the cross-section is: $\mathrm{I}_{\mathrm{Gz}}=\frac{1}{12}L.e^3$ 2.4
  compared to the (G, Z) axis
- R : radius of curvature average.

The application of the theorem of Castigliano [3] at the point C : where U is the energy of deformation ; makes it possible to establish the relation Y_C = a.P with

$$\mathrm{a} = \frac{R}{4ES}\left[\left(\frac{\pi}{2}-\theta_1\right)+\frac{1}{2}\sin 2\theta_1\right]+\frac{R}{4GS}\left[\frac{\pi}{2}-\theta_1-\frac{1}{2}\sin(2\theta_1)\right]+$$
$$\frac{R^3}{2EI_{Gz}}\left[\left(\frac{\pi}{2}-\theta_1\right)\cos^2\theta_1-2\cos\theta_1+\frac{3}{4}\sin 2\theta_1+\frac{1}{2}\left(\frac{\pi}{2}-\theta_1\right)\right] \qquad 2.5$$

Knowing that $G=\dfrac{E}{2(1+\nu)}$

To simplify equation (2.5) we note $\mathrm{a} = \dfrac{1}{\mathrm{E}}\left[\alpha+(1+\nu)\beta+\gamma\right]$ 2.6

with

$$\alpha = \frac{R}{4S}\left[\left(\frac{\pi}{2}-\theta_1\right)+\frac{1}{2}\sin 2\theta_1\right] \quad \beta = \frac{R}{2S}\left[\frac{\pi}{2}-\theta_1-\frac{1}{2}\sin(2\theta_1)\right]$$

$$et \quad \gamma = \frac{R^3}{2EI_{Gz}}\left[\left(\frac{\pi}{2}-\theta_1\right)\cos^2\theta_1-2\cos\theta_1+\frac{3}{4}\sin 2\theta_1+\frac{1}{2}\left(\frac{\pi}{2}-\theta_1\right)\right] \qquad 2.7$$

The identification of a_1 and a gives equation (2.8) where the only unknown factors are E and ν.

We have thus: $\mathrm{a}_1 = \dfrac{1}{\mathrm{E}}\left[\alpha+(1+\nu)\beta+\gamma\right]$ 2.8

Relation (2.8) above utilizes at the same time two unknown factors E and ν. The knowledge of the slope a_1 is insufficient to determine E and ν, it is necessary to determine another relation. This one is obtained from the elastic test of penetration of Hertz (indentation test).

b-2 Indentation test

b-2-1 Experimental data-gathering

We propose to exploit the elastic contact theories of Hertz [15]. We consider the case of an elastic contact between steel balls spherical of ray R_2 and of a plane sample of coconut shell. The principle of the elastic contact test is illustrated by the diagram of figure 8, of the device which we designed and realized for this purpose, in the case of a contact sphere-plane.

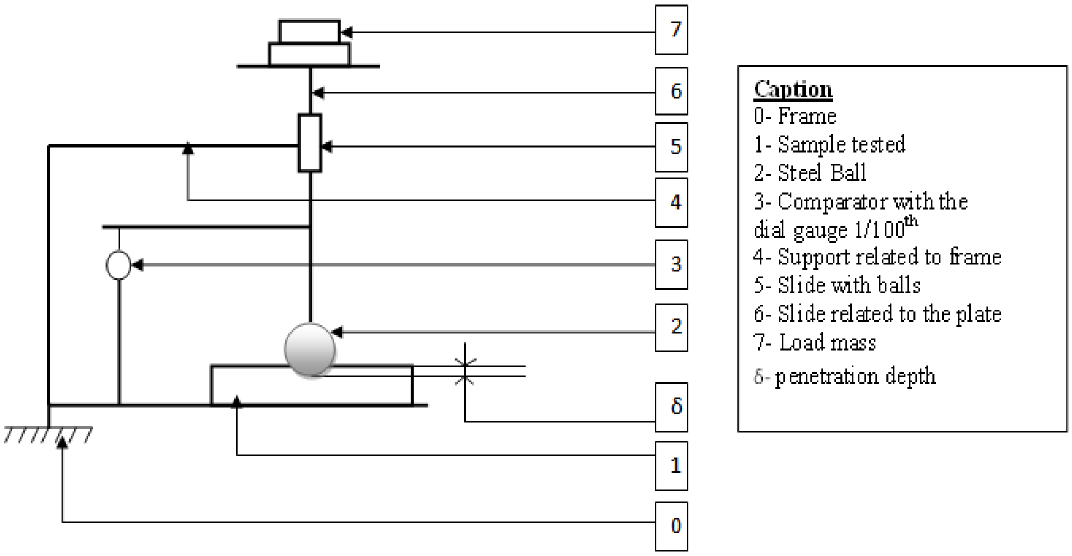

Figure 8: Diagram of the indentation test

The sample of coconut shell 1 with plane and parallel faces, is laid out on a plane surface and horizontal related to frame 0. The steel ball 2 in contact with the sample is related to slide 6 interdependent of the plate receiving mass 7. The slide-plate unit and mass are guided in translation in the vertical direction by slide 5 interdependent of the frame. The sensor button of the dial gauge to the $1/100^{th}$ makes it possible to read the interpenetration δ of 2 in 1. It is admitted that the stem is perfectly rigid. The data-gathering for a sample is done by the statement of the couples of the values: charge P and corresponding penetration δ. We thus tested more than 20 samples coming from the two species from shell and for each sample we carried out 8 experimental points. We make sure that the assumptions of Hertz are respected during tests. The figure 9 gives the curve of the cube δ according to the squared of P for species 1.

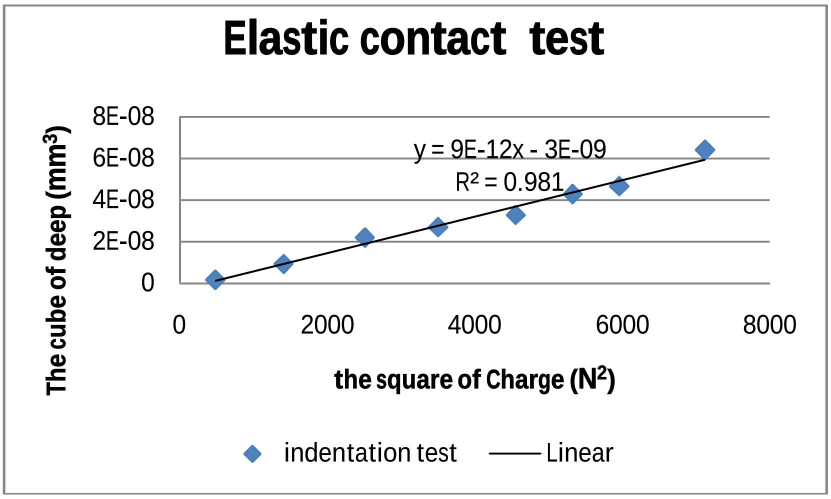

Figure 9: Elastic contact test

b-2-2 Exploitation of the experimental data

The theory of Hertz, with regard to the elastic contact, gives us the total interpenetration $\delta = \delta_1 + \delta_2$ of the two solids in contact. However solid 2 (steel ball) being supposed perfectly rigid, compared to the coconut shell, we admit that the total deflection of the two solids is summarized with that of solid 1 (sample of shell). From where $\delta = \delta_1$

According to this theory [14] $\delta = \left(9Fz^2 / 16RE^{*2} \right)^{1/3}$ 2.9

where we have $\delta^3 = \frac{9}{16RE^{*2}} F_z^{\ 2}$ 2.10

With $\frac{1}{E^*} = \frac{1-\nu_1^{\ 2}}{E_1} + \frac{1-\nu_2^{\ 2}}{E_2}$ 2.11

and $\frac{1}{R} = \frac{1}{R_1} + \frac{1}{R_2}$ 2.12

since R_1 tends towards the infinite and E_2 is very large compared to E_1 then $R = R_2$ and

$$\frac{1}{E^*} = \frac{1-\nu_1^{\ 2}}{E_1} \qquad 2.13$$

To exploit the experimental data, we identify the coefficient of the linear straight regression line of the experimental data which we note a_2 with the theoretical proportionality factor between the cube of depth δ with the squared of load F_z.

From where the equation $a_2 = 9/16RE^{*2}$ 2.14

$$a_2 = \frac{9}{16R_2\left(\frac{E}{1-\nu_1^{\ 2}}\right)^2} \Rightarrow E = \sqrt{\frac{9}{16R_2 a_2}} * \left(1-\nu_1^{\ 2}\right) \qquad 2.15$$

which gives:

Let $\mathrm{E} = \mathrm{C}\left(1 - \nu_1^{\ 2}\right)$ 2.16

with $\mathrm{C} = \sqrt{\frac{9}{16\mathrm{R}_2 a_2}}$ 2.17

The second equation is obtained: $\mathrm{E} = \mathrm{C}\left(1 - \nu_1^{\ 2}\right)$ 2.18

In the continuation we take $\nu_1 = \nu$

b-3 Estimate of the Young modulus E and the Poisson's ratio ν

Equations (2.8) and (2.18) form a system of 2 equations with unknown factors E and ν.

$$\begin{cases} a_1 E = \alpha + \left(1-\nu^2\right)\beta + \gamma \\ E = C\left(1-\nu^2\right) \end{cases} \qquad 2.19$$

$$(2.18) \text{ in } (2.8) \text{ gives } \quad a_1 C\left(1-\nu^2\right) = \alpha + \left(1+\nu\right)\beta + \gamma \qquad 2.20$$

From where the second degree polynomial of ν: $a_1C\nu^2 + \beta\nu + (\alpha + \beta + \gamma) = 0$ 2.21

The determinant is: $\Delta=\beta^2 - 4a_1C\,(\alpha+\beta+\gamma-a_1C)$. In the case that Δ is positif, there will be two solutions

$$\nu_1 = \frac{-\beta - \sqrt{\Delta}}{2a_1C}; \nu_2 = \frac{-\beta + \sqrt{\Delta}}{2a_1C} \qquad 2.22$$

For each value of ν corresponds a value of E following the equation (2.8).

3- Results, discussion and comparison

3-1 Results

3-1-1 Physico-chemical properties of coconut shells

- The average values of densities of the coconut shells are given in table 3.

  Table 3: Experimental values of the densities of species 1 and 2 of coconut

Species	ρ (kg/m^3)	Δρ (kg/m^3)
1	1211	46.34
2	1244	56.34

- The SEM of coconut shell, obtained with an enlargement ×200, is given in figure 10. It can be observed that the physical structure of the coconut shells is granular and the grains are lengthened in the southernmost direction.

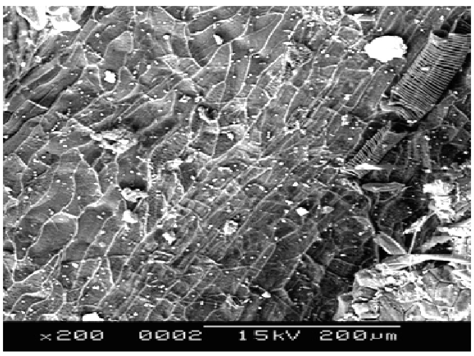

Figure 10: Structure of the shell of coconut seen under the Electronic

- The FTIR curve of the coconut shell analysis is given in figure 11. The FR analysis of those shell on a tape wavelengths is from 600 cm^{-1} to 3900 cm^{-1}; emphasized on the several peaks of which most significant are with 3340.54cm^{-1}, 2919.95cm^{-1}, 1730.84cm^{-1}, 1593.99cm^{-1}, 1509.65cm^{-1}, 1371.43 cm^{-1}, 1236.82 cm^{-1}, 1162.9 cm^{-1}, 1032.87 cm^{-1}. Characteristic and prominent peaks are assigned in the table 7 where we summarize the main part of information on the chemical bonds and some functional groups. The results obtained by Andrzej K and all [7] on FT-IR technique presented in table 4 are similar to ours.

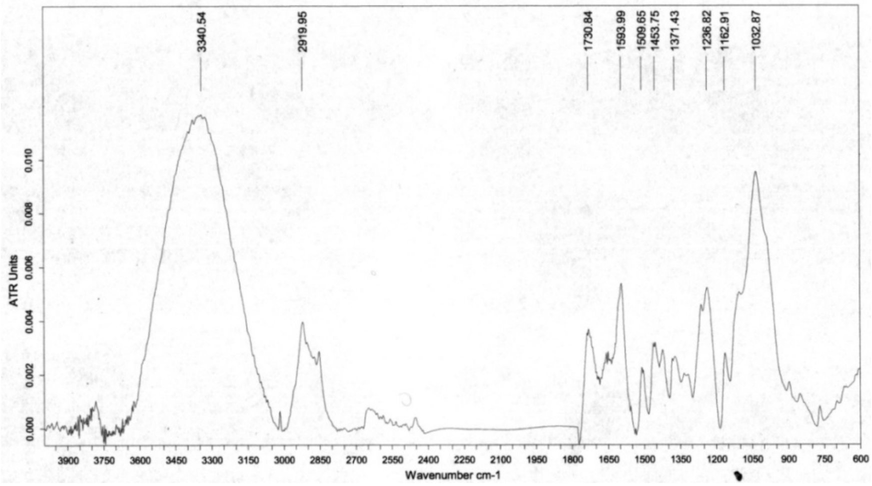

Figure 11: FTIR curve of analysis of the coconut shell

Table 4: analyze spectrometric FT-IR of the coconut shell [7]

Peak location range (cm^{-1})	Assignment
3401	O-H Stretching
2911	C-H asymmetric and symmetric stretching in methyl and methylene group
2326	P-H stretching and P-O-H stretching
2106	Si-H Stretching
1721	C=O stretching in acetyl and uronic ester groups or in carboxylic group of ferulic and coumaric acids
1621	N-H bending in primary amine
1371	C-H rocking in alkanes or C-H stretching in methyl and phenolic alcohol
1249	Liaison C-C plus C-O plus C=O
1032	C-O deformation in secondary alcohol and aliphatic ether or aromatic
893	C-I group frequency or ring frequency

- The TGA curve of coconut shell is given in figure 12. The TGA analysis of the coconut shell, for temperatures going up to 800 °C, gives us the volatiles elements, the rate of ash contents in the coconut shell. Decomposition took place in three major mass loss steps as follows:

- Between 0°C and 150° C, 7.625 % corresponding to loss of water;
- Between 250° C and 420° C, 51.75 %, corresponding to loss of volatiles from the hemicelluloses, cellulose and lignin present;
- Between 450°C and 700°C, 39.56% loss of skeletal carbon;
- The residual mass at 800°C was very low, representing less than 1% by weight of analyzed sample indicating very low ash content. The relative low temperature of volatisation was observed

This analysis was made by Andrzej and all [7] but for temperatures of about 300°C as shown in the figure 13.

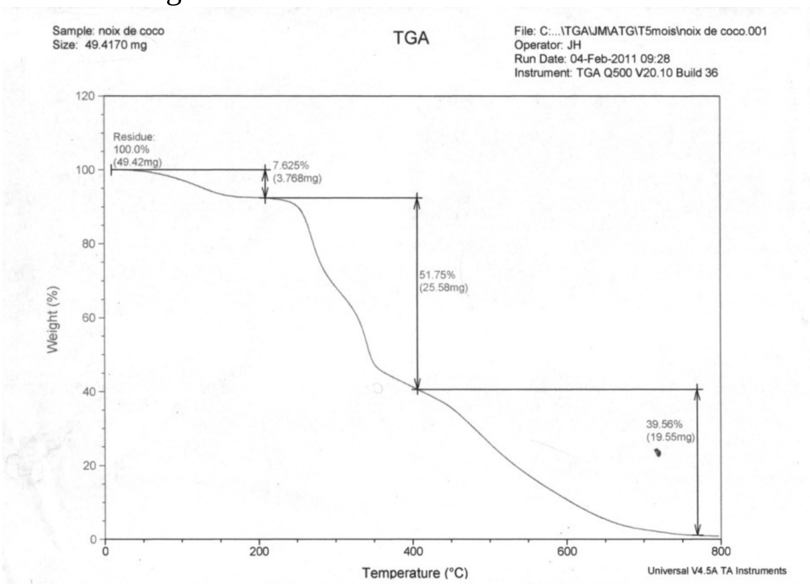

Figure 12: Curve of the TGA of the coconut shell

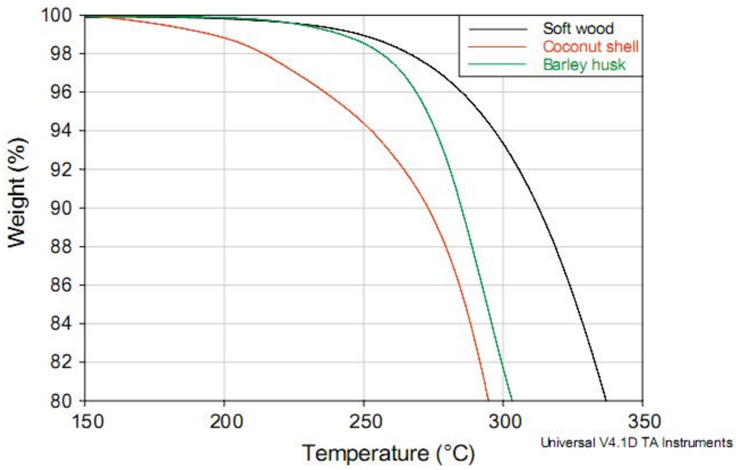

Figure 13: Curves of thermo gravimetry [4]

3-1-1 Mechanical properties

- The average values of impact strengths of the samples of coconut shell at room temperature is given in table 5. His energy of impact lies between 1.76 and 1.9 J/cm^2 for species 1 and between 1.92 and 2.11 J/cm^2 for species 2. Its value in the polar zone is slightly larger than that of the equatorial zone on coconut. This energy of impact strength decreases almost in linear way according to temperature going from 25°C with 137°C. It is practically divided by four when the temperature increases from 25° C to 137°C as shown in figure 14.

Table 5: Average values of impact strengths of the right samples of coconut shells at room temperature

Species	Type of Samples	Average values of the impact strengths in j/cm^2	Species	Type of Samples	Average values of the impact strengths in j/cm^2
1	1ZE-S	1.78	2	2SE-S	1.94
1	1ZE-E	1.85	2	2ZE-E	3.13
1	1ZP-S	1.94	2	2ZP-S	2.11
1	1ZP-E	1.77	2	2ZP-E	1.94
Average		1.83	Average		2.02
Standard deviation		0.07	Standard deviation		0.01

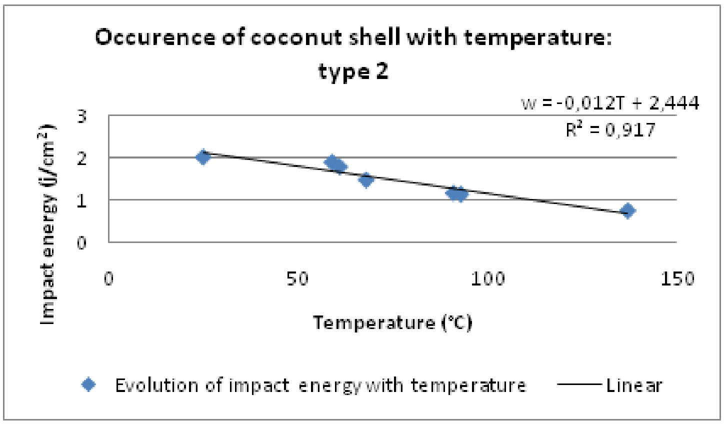

Figure 14: Curve of variation of impact strengths of the coconut shells of the type 2 according to the

- The 3 points flexural test till rupture as shown in figure 15 has proved that coco nut shell can be consider as ductile material.

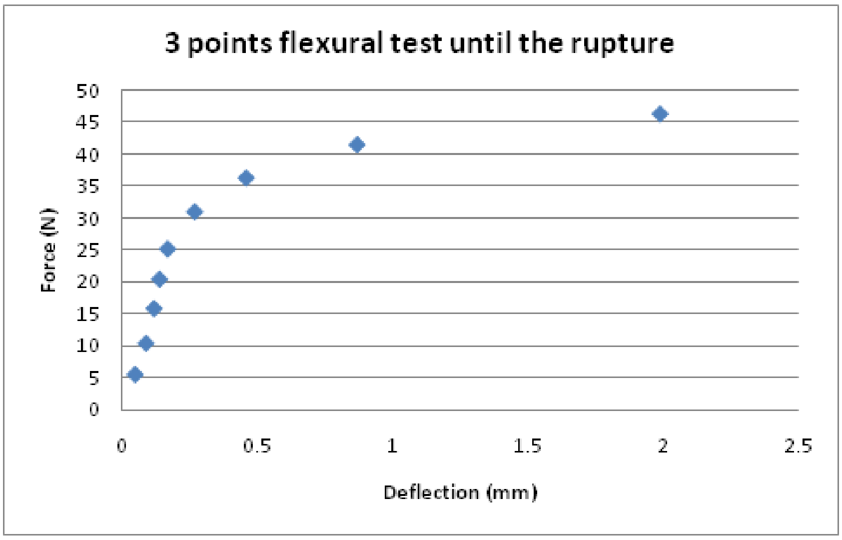

Figure 15: 3 points deflection test until the rupture

- The phenomenon of hysterisy was observed for these shells as the curve of unloading of the 3 points flexural tests shown in figure 7.
- The values of Young modulus and Poisson ratio of all the samples of coconut shell are present in table 7. The average values of static Young modulus and Poisson's ratio obtained following the species and the orientation are given in tables 6, 7 and 8.

Table 6: Values of Young Modulus and Poisson's ratio of the coconut shells obtained

Samples Species 2	Poisson ratio ν	Young modulus E (MPa)	Samples Species 1	Poisson ratio ν	Young modulus E (MPa)
Samples cut in the equatorial direction					
2 E1	0,86	19789	1 E1	0,91	12695
2 E2	0,93	10244	1 E2	0,93	10816
2 E3	0,89	16044	1 E3	0,91	12701
2 E4	0,92	12256	1 E4	0,93	10430
2 E5	0,89	15227	1 E5	0,92	10997
2 E6	0,92	11353	1 E6	0,92	11390
2 E7	0,91	13351	1 E7	0,91	12828
2 E8	0,92	11428	1 E8	0,91	12455
2 E9	0,90	13929	1 E9	0,91	12593
2 E10	0,92	11477	1 E10	0,91	11879
Moy	0,91	13510	Moy	0,92	11878
Ecart	0,02	2874	Ecart	0,01	957
Samples cut in the southernmost direction					
2M1	0,90	14469	1M1	0.86	20360
2M2	0,87	18199	1M2	0,85	21275

2M3	0,83	23578	1M3	0.84	20348
2M4	0,87	18932	1M4	0,84	22772
2M5	0,87	19204	1M5	0.84	20348
2M6	0,90	14237	1M6	0,85	21034
2M7	0,86	19189	1M7	0.85	20354
2M8	0,83	23861	1M8	0,89	16336
Moy	0,86	18958	Moy	0,85	20353
Ecart	0,03	3555	Ecart	0,02	1825

Table 7: Values of the static Young modulus of the coconut shells

	Species 1	Species 2
Equatorial direction	[10921 ; 12835] in MPa	[10636 ; 16384] in MPa
Southernmost direction	[18528 ; 22178] in MPa	[15403 ; 22513] in MPa

Table 8: Values of the Poisson's ratios of the coconut shells

	Species 1	Species 2
Equatorial direction	[0.91 ; 0.93]	[0.89 ; 0.93]
Southernmost direction	[0.83 ; 0.87]	[0.83 ; 0.89]

3-2 Discussion and comparison

- The chemical elements and functions which enter the composition of this shell were highlighted by the spectrometric analysis. These functions are conforms to the chemical composition [9] of these shells such as present table 9.

Table 9: Chemical composition of the coconut shells [9]

Composition (%)	Coconut shells
Cellulose	34 %
Hemicellulose	21 %
Lignin	27 %

- The static Young modulus of these shells in equatorial direction (E) is not the same one in the southernmost direction (M). This anisotropy can be justified by the directed granular structure of the coconut shell which we observed on figure 10. In fact it appears clearly that his structure is granular and grains are lengthened in the southernmost direction.
- Table 10 gives us a comparison of the specific rigidity of the coconut shells with other materials. It is deduced from this table that coconut shells are specifically:
  - More rigid than the majority of the polymers (Polyethylene, epoxy Polycarbonate, poly, Poly ester, etc.);
  - Close relations of certain materials very much used like steels, Aluminum and Zirconium.

- It appear clearly from table 11 that coconut shell are more rigid than most of the wood.
- The Poisson's ratios of these shells are very close to those of certain woods, for example the Poisson's ratio the one call “peuplier” is around 1.04 [18]. Moreover this wood has a granular structure near to that of the coconut shells and its characteristics were determined by a technique of observation with weak enlargement of the surface of a small sample subjected to an increasing elongation [18].

Table 10: comparison of specific rigidities [16]

Materials	Density En t/m^3	Young modulus in GPa at 25°C	Specific rigidity in GPa.m^3/t
Aluminium	2.7	71	26.3
Bore	2.63	400	152
Béryllium	1.8	315	175
Magnésium	1.74	42	24.1
Titane	4.51	120	26.6
Acier	7.8	210	26.9
Tungstène	19.3	411	21.3
Zirconium	6.49	94	14.5
Polyéthylène	0.93	0.2	0.2
Polycarbonate	1.30	2.4	1.8
Poly époxyde	1.3	2.4	1.8
Polyester	1.35	5	3.7
COCONUTS SHELLS			
Southernmost direction	1.2	19,8	14,4
Equatorial direction	1.2	12,7	10,6

Table 11: Comparison of rigidity with some wood [18]

Wood	
Species	Young modulus (MPa)
Sapin épicea	9,6
Pin	11,0
Douglas	11,8
Eucalyptus saligna	14,7
COCONUTS SHELLS	
Southernmost direction	19,8
Equatorial direction	12,7

Conclusion

This work enabled us to determine the mechanical characteristics and physic-chemical property of coconut shells nucifera in maturity of Cameroon, and mainly those of two varieties. The coconut shells which were the subject in this study are taken in nature and are preserved at the ambient temperature. We set up the experimental devices to determine in the one hand: their density; the chemical elements content; the volatiles elements and the rate of ash contents. Its physical structure has also been observed and it is granular and the grains are lengthened in the southernmost direction of nut. In the other hand, we determine the mechanical characteristics of these shells, such as: their energy of impact strength; their static Young modulus and their Poisson's ratio. These studies show us that the coconut shells are denser than water and their densities vary between 1211 and 1244 kg/m3. Their energy of impact strength varies from 1,83 to 2,02 J/cm² and it decreases with temperature in an almost linearly. It is practically divided by four when the temperature increases from 25° C to 137°C. In appear clearly those shells are anisotropic materials and seem to be ductile.

REFERENCES

[1] KAPSEU, C., JUILLET-DÉCEMBRE 2009, ”Production, analyse et applications des huiles végétales en Afrique,” CONFÉRENCE CHEVREUL, OCL VOL. 16 N° 4.

[2] Selvan, A., Nair, N. G., Paramanand Singh., 1998, “Synthesis and characterisation of SiC whiskers from coconut shell,” Journal of Materials science N° 17, 57-60.

[3] Krista, S. W., Celio, L. C., and M. Douglas, L., 2005, ”Adsorption Equilibrium of Alkanes on a high Surface Area Activated carbon prepared from brazilian Coconut Shells,” Science+Business Media 11, 107-111.

[4] Rafael, B. R., Wilton, F., Silva, M., Eurico, A., Torres, B., Diana, C.S., Azervedo, Célio L. C., 2009, ”Absorption of methane in actived carbons obtained from coconut shells H_3PO_4 chemical activation,” Science+Business Media, N°15, 271-277.

[5] Shrikant, A., Survase, Bacigalupi. C., Uday, S., Annapure, and Singhal, S., 2009, ”Use of Coconut Coir Fibers as an Inert Solid Support for Production of Cyclosporin A,” Biotechnology and Bioprocess Engineering., N°14: 769-774

[6] Olontsev, V. F., Borisova, I.A., and Sazonova, E. A., 2011, ”Pyrolysis of Coconut Shells for the Manufacture of Carbon Sorbents,” Solid Fuel Chemistry, Vol. 45, No. 1, pp. 44–49

[7] Andrzej K., Bledzki, Abdullah A., Mamun, Jürgen Volk, 2010, ”Barley husk and coconut shell reinforced polypropylene composites: The effect of fibre physical, chemical and surface properties,” Journal of Composites Science and Technology 70, pp. 840-846.

[8] Sarki, J., Hassan, S.B., Aigbodion, V.S., Oghenevweta, J.E., 2011, ”Potential of using coconut shell particle fillers in eco-composite materials,” Journal of alloys and compounds, 509, pp. 2381-2385.

[9] Gunasekaran, K., Kumar, P.S., Lakshmipathy, M., 2011, ”Mechanical and bond properties of coconut shell concrete,” Construction and Building Materials 25, pp. 92-98.

[10] Husseinsyah, S., and Mostapha@ Zakaria, M., 2011, ”The effect of Filler on properties of Coconut Shell Filled Polyester Composites,” Malaysian Polymer Journal, vol. 6, N° 1, p. 87-97.

[11] TAYLOR, J., 2000, ”Incertitudes et analyse des erreurs physiques,” Dunod, Masson Sciences.Liège, 345 pages.

[12] Sapuan, S.M., Harini, M., Maleque, M.A., 2003, “Mechanical properties of epoxy/coconut shell filler particles composites,” The Arabian Journal for science and Technology, vol. 28, N° 2B.

[13] NOUGIER, J.P., 1985, ”Méthodes de calcul numérique,” ; Ed. MASSSON, 254 pages.

[14] BAZERGUI, A., Thang BUI-QUOC, D., MCINTYRE, M., LABERGE, C., 1993, ”Résistance des matériaux,” 2ème édition de l’Ecole Polytechnique de Montréal.

[15] GEORGES, J.M., 2000, ”frottement, usure et lubrification, tribologie ou sciences des surfaces,” Eyrolles, Paris, 424 pages.

[16] DORLOT, J.M., BAÏLON, J.P., MASSOUNAVE, J., 1986, ”Des matériaux, ” 2ème édition revue et augmentée de l’Ecole Polytechnique de Montréal.

[17] Marchal, P., 2009, ”Essais mécaniques sous microscopique,” INRA – UMR1092 – Numéro spécial.

[18] MUKAM FOTSING, J. A., 1990, ”Modélisation statistique du comportement mécanique du matériau bois. Application à quelques Essences du Cameroon, ” Mémoire de thèse. Université de Yaoundé.

APPENDIX
EXPRESSION OF THE TOTAL ENERGY OF DEFORMATION OF THE STRUCTURE

The 3 points flexural test is carried out on a curved beam having the form of a portion of cylinder such as the figure shown below.

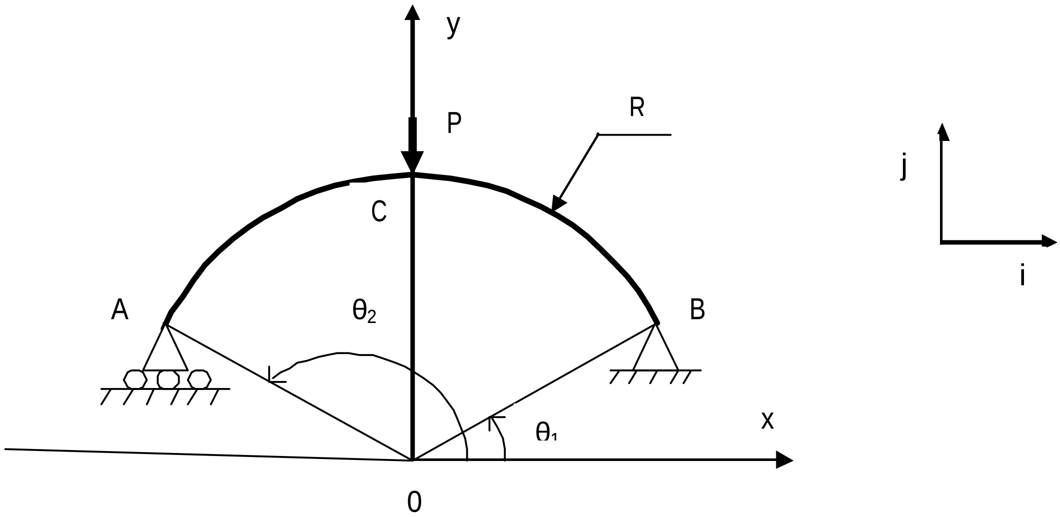

Figure A-2: Mathematical model of the flexural test in three points

The equilibrium of the beam led to the determination of the reactions R_A and R_B respectively to supports A and B. We obtain then $\vec{R}_A = \vec{R}_B = \dfrac{P}{2}\vec{j}$

To determine the torque of the efforts of cohesion in the centre of gravity of the cross-section, we make a fictitious cut between the points A and C; and we preserve the part of left.

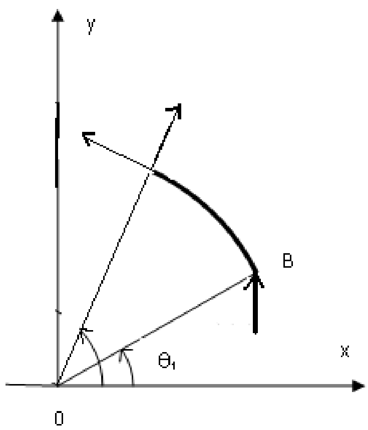

Figure A-3 Equilibrium of the left part

The torque of the efforts of cohesion in the centre of gravity G of the cross-section is defined as:

$$\begin{Bmatrix} \vec{R} \\ \vec{M}_G \end{Bmatrix} \text{ with } \begin{cases} \vec{\mathrm{R}} = \mathrm{N}\,\vec{\mathrm{e}}_\theta + T_R \vec{e}_R + T_z \vec{k} \\ \vec{\mathrm{M}}_\mathrm{G} = Mt\ \vec{e}_\theta + Mfr\ \vec{e}_R + Mfz\ \vec{k} \end{cases}$$

Where $\begin{cases} \vec{\mathrm{e}}_\theta = \sin\theta\,\vec{i} - \cos\theta\,\vec{\mathrm{j}} \\ \vec{e}_R = \cos\theta\,\vec{\mathrm{i}} + \sin\theta\,\vec{\mathrm{j}} \end{cases}$ in the same way $\begin{cases} \vec{\mathrm{i}} = \sin\theta\,\vec{\mathrm{e}}_\theta + \cos\theta\,\vec{\mathrm{e}}_\mathrm{R} \\ \vec{j} = -\cos\theta\,\vec{\mathrm{e}}_\theta + \sin\theta\,\vec{\mathrm{e}}_\mathrm{R} \end{cases}$

The equilibrium of the section (figure A-2) gives:

$$\begin{cases} \mathrm{N} = \dfrac{\mathrm{P}}{2}\cos\theta \\ T_R = -\dfrac{P}{2}\sin\theta \\ Tz = 0 \end{cases} \text{ and } \begin{cases} Mt = 0 \\ Mfr = 0 \\ Mfz = \dfrac{RP}{2}\left(\cos\theta_2 - \cos\theta\right) \end{cases}$$

We indicate by:

- U_1: the deformation energy due to N;
- U_2 the deformation energy due to T_R;
- U_3 the deformation energy due to Mf_z;
- U: the total deformation energy.

$$U_1 = \frac{1}{2}\int_V \sigma\varepsilon dv \text{ with } \sigma\varepsilon = \frac{1}{E}\left(\frac{N}{A}\right)^2$$

$$\mathrm{U}_1 = \frac{RP^2}{8EA}\int_{\frac{\pi}{2}}^{\theta_2}\cos^2\theta\,\mathrm{d}\theta \Rightarrow \mathrm{U}_1 = \frac{\mathrm{RP}^2}{8\mathrm{EA}}\left(\theta_2 + \frac{1}{2}\sin 2\theta_2 - \frac{\pi}{2}\right)$$

$$U_2 = \frac{1}{2}\int_V \tau\gamma dV \text{ with } \tau\gamma = \frac{1}{\mathrm{G}}\left(\frac{T_R}{A}\right)^2 \text{ où } \mathrm{T_R} = -\frac{\mathrm{P}}{2}\sin\theta$$

$$\mathrm{U}_2 = \frac{RP^2}{8GA}\int_{\frac{\pi}{2}}^{\theta_2}\sin^2\theta\,\mathrm{d}\theta \Rightarrow \mathrm{U}_2 = \frac{RP^2}{16GA}\left(\theta_2 - \frac{1}{2}\sin 2\theta_2 - \frac{\pi}{2}\right)$$

$$U_3 = \frac{1}{2}\int_V \sigma\varepsilon\, dV \quad \text{with} \quad \sigma\ \varepsilon = \frac{1}{\mathrm{E}}\left(\frac{Mfz}{I_{Gz}}y\right)^2 \quad ; \ \mathrm{dV} = \mathrm{dxdA}$$

knowing that $\mathrm{I_{Gz}} = \int_{\mathrm{A}} \mathrm{y}^2 \mathrm{dA}$ and that $\mathrm{Mfz} = \dfrac{\mathrm{RP}}{2}\left(\cos\theta_2 - \cos\theta\right)$

from where $\mathrm{U}_3 = \dfrac{\mathrm{R}^3 P^2}{8EI_{Gz}}\displaystyle\int_{\frac{\pi}{2}}^{\theta_2}\left(\cos\theta_2 - \cos\theta\right)^2 \mathrm{d}\theta$

$$\Rightarrow \quad \mathrm{U}_3 = \frac{\mathrm{R}^3 P^2}{8EI_{Gz}}\left[\left(\theta_2 - \frac{\pi}{2}\right)\left(\cos^2\theta_2 + \frac{1}{2}\right) - \frac{3}{4}\sin 2\theta_2 + 2\cos\theta_2\right]$$

The expression of the total deformation energy of the beam is:

$$\mathrm{U} = 2\left(\mathrm{U}_1 + U_2 + U_3\right)$$

$$\Rightarrow \quad \mathrm{U} = \frac{\mathrm{RP}^2}{4\mathrm{EA}}\left(\theta_2 + \frac{1}{2}\sin 2\theta_2 - \frac{\pi}{2}\right) +$$

$$\frac{RP^2}{8GA}\left(\theta_2 - \frac{1}{2}\sin 2\theta_2 - \frac{\pi}{2}\right) +$$

$$\frac{\mathrm{R}^3 P^2}{4EI_{Gz}}\left[\left(\theta_2 - \frac{\pi}{2}\right)\left(\cos^2\theta_2 + \frac{1}{2}\right) - \frac{3}{4}\sin 2\theta_2 + 2\cos\theta_2\right]$$